Structural Engineering and Mechanics, *Vol. 70, No. 5 (2019) 623-637*
DOI: https://doi.org/10.12989/sem.2019.70.5.623

Non-stationary vibration and super-harmonic resonances of nonlinear viscoelastic nano-resonators

Masoud Ajri[a], Abbas Rastgoo[b] and Mir Masoud Seyyed Fakhrabadi[*]

School of Mechanical Engineering, College of Engineering, University of Tehran, Tehran, Iran

(Received April 9, 2018, Revised October 23, 2019, Accepted March 12, 2019)

Abstract. This paper analyzes the non-stationary vibration and super-harmonic resonances in nonlinear dynamic motion of viscoelastic nano-resonators. For this purpose, a new coupled size-dependent model is developed for a plate-shape nano-resonator made of nonlinear viscoelastic material based on modified coupled stress theory. The virtual work induced by viscous forces obtained in the framework of the Leaderman integral for the size-independent and size-dependent stress tensors. With incorporating the size-dependent potential energy, kinetic energy, and an external excitation force work based on Hamilton's principle, the viscous work equation is balanced. The resulting size-dependent viscoelastically coupled equations are solved using the expansion theory, Galerkin method and the fourth-order Runge–Kutta technique. The Hilbert–Huang transform is performed to examine the effects of the viscoelastic parameter and initial excitation values on the nanosystem free vibration. Furthermore, the secondary resonance due to the super-harmonic motions are examined in the form of frequency response, force response, Poincare map, phase portrait and fast Fourier transforms. The results show that the vibration of viscoelastic nanosystem is non-stationary at higher excitation values unlike the elastic ones. In addition, ignoring the small-size effects shifts the secondary resonance, significantly.

Keywords: viscoelasticity; non-stationary motion; nonlinear dynamic; super-harmonic resonance; nano-resonator

1. Introduction

Micro-nanoelectromechanical devices (MEMS-NEMS), due to their accuracy and ultra-high sensitivity are widely used in research areas relating to the spin detection (Budakian *et al.* 2006, López 2013), mass detection (Yang *et al.* 2006, Li *et al.* 2007, Naik *et al.* 2009), damage detection (Shinozuka *et al.* 2010, Domaneschi *et al.* 2013), coupled resonance (Sato *et al.* 2003, Shim *et al.* 2007, Huber *et al.* 2010) and biochemistry (Leng and Lin 2011, Hwang *et al.* 2017, Pan and Chen 2017). Micro-nanomechanical resonators are a main branch of these devices highlighted for their excessive frequency (Huang *et al.* 2005, Baghelani 2016). Better detection of the physical quantities by these resonators highly depends on characterizing their dynamic behavior, accurately (Ekinci *et al.* 2004, Braun *et al.* 2005, Tajaddodianfar *et al.* 2017). Therefore, it is necessary to illustrate and realize their dynamic characteristics to design new sensing instruments. Clearly, the dynamic characteristics of these resonating devices are highly influenced by their specific mechanical properties such as elasticity and viscoelasticity. Recently, some new experiments showed that the viscoelastic properties extensively present in materials such as silicon (Elwenspoek and Jansen 2004) and polysilicon (Teh and Lin 1999) used widely in MEMS/NEMS. Moreover, the viscoelastic characteristics of graphene oxide layers were demonstrated by tensile tests on these plates (Su *et al.* 2012). Furthermore, the viscoelastic properties of the nanostructures were also studied (Karlicic *et al.* 2014, Mohammadimehr *et al.* 2015, Khaniki and Hosseini-Hashemi 2017). Recently, Ajri *et al.* (2018a, 2018b) studied the viscoelasticity effects on the nonlinear dynamics of a viscoelastic nano-plate.

Experimental results revealed that the viscoelasticity effects significantly influence the system behavior (Elwenspoek and Jansen 2004, Tuck *et al.* 2005). In general, in viscoelastic structures, a part of deformation energy is recoverable where the other part is not. The irrecoverable part of the deformation energy produces thermally actuated mechanical fluctuations and the frequencies of oscillators are highly influenced by the viscoelastic dissipation (Saulson 1990, Paolino and Bellon 2009). As a result, it is necessary to consider the viscous dissipation in dynamic analysis of the nano-resonators.

In addition to the less-concentrated viscoelasticity in formulating the deformation of micro and nanostructures, the small-scale effects play very crucial roles. Many researchers all around the world investigate the different mechanical properties of the micro-nanostructures by applying the classical continuum theories. However, as mentioned at the micro-nanoscales, the surface and size effects often become noticeable that cannot be disregarded. Experimental findings and atomistic simulations showed significant size-effects (Mindlin and Tiersten 1962, Jiang *et*

*Corresponding author, Assistant Professor
E-mail: mfakhrabadi@ut.ac.ir
[a] Ph.D. Student
E-mail: m.ajri@ut.ac.ir
[b] Professor
E-mail: arastgo@ut.ac.ir

ISSN: 1225-4568 (Print), 1598-6217 (Online)

al. 2009) on the mechanical properties at micro-nanoscales. The small-scale effects usually increase the stiffness of the nanostructures and the stiffness changes the dynamic behavior of these elements, remarkably. Classical continuum models are supposed to be scale-free, so their application leads to inaccurate results. In order to compensate the lacks of the size-independent classical concepts, several theories taking the size effects have been introduced (Toupin 1962, Gurtin and Murdoch 1975, Aifantis 1999, Yang *et al.* 2002, Lam *et al.* 2003) for the elastic materials. One of the most important size-dependent continuum models is the modified couple stress theory (MCST) (Yang *et al.* 2002) used in this paper. In this theory, when the couples, couples moments and applied forces resultant have zero values, the materials reach the equilibrium state. The MCS theory was applied to examine the mechanical behavior of the elastic micro-nanostructures such as vibration (Babaei *et al.* 2017, Ehyaei and Akbarizadeh 2017, Ghadiri *et al.* 2017, Setoodeh and Rezaei 2017), nonlinear dynamics (Akbas 2016, Park *et al.* 2016, Ghayesh *et al.* 2017) and electromechanical characteristics (Ghayesh *et al.* 2013, Kalyanaraman *et al.* 2013).

The literature regarding the static and dynamic size-dependent behavior of the micro-nanoplates with elastic model is relatively wide. For example, based on the MCST for linear case, Ma *et al*. (2011) analyzed the static and free vibration of the microplates using the first-order shear deformation plate model. Furthermore, Ke *et al.* (2012) and Jomehzadeh *et al.* (2011) applied the MCS theory to study the free linear vibrations of Mindlin and Kirchhoff microplates. For the nonlinear case, Asghari (2012) applied the MCST to study the size-dependent nonlinear motion of the microplates. However, despite the extensive research on the viscoelastic models at the macro-scales (Mockensturm and Guo 2005, Ghayesh and Amabili 2012, Tang and Chen 2012), the large amount of literatures on the dynamics/statics of micro-nanostructures are on the base of the elastic model. Recently, a number of researchers considered the viscoelastic models on dynamic/static modeling of the micro-nanostructures. For example, Ebrahimi and Hosseini (2016) studied the viscoelasticity effects on vibration behavior of a nanoplate with viscoelastic material in thermal environments. Liu *et al.* (2017) investigated the vibration of a viscoelastic functionally Graded nanoplate. In addition, Jamalpoor *et al*. (2017) discussed the out-of-plane vibration of a orthotropic multi-layer microplate with viscoelastic material via the modified strain gradient theory. In all of the mentioned studies, no solutions were provided for the nonlinear dynamics of viscoelastic micro-nanoplates and only the equations of motion were achieved and reported. Moreover, the mentioned studies used the Kelvin-Vigot material, allowing modeling the linear viscoelasticity while many viscoelastic materials do not have linear behavior clearly showing nonlinear mechanical responses. In order to solve this problem, an evaluation study (Smart and Williams 1972) revealed that the nonlinear Leaderman relation (Leaderman 1962) is useful when prediction and easiness are important. The recent paper studies the viscoelastically coupled nonlinear dynamics of a plate-shape nano-resonator made of the viscoelastic material following the Leaderman integral nonlinear relation.

To the best of the author's knowledge, there is no study in the previous literature that examines the free vibration and nonlinear forced vibration of the viscoelastic nano-resonators including secondary resonance. This paper analyzes the time-dependent natural frequencies and secondary resonance in super-harmonic motions of a viscoelastic nano-resonator. The resonator is assumed as a nanoplate with simply supported boundary conditions. Then, a new coupled size dependent model is developed for viscoelastic material with using the MCS theory. In order to capture the system oscillative behavior at relatively large deformations, the von-Karman theory is considered in this model. The virtual work induced by the viscous forces calculated with using the Leaderman integral. With incorporating the size-dependent potential energy, kinetic energy, and an external excitation force work based on the Hamilton's principle, the viscous work equation is balanced. The obtained coupled equations are a set of nonlinear second order integro-differential partial equations. These equations are converted to Duffing equation by applying expansion theory. The coupled nonlinear Duffing and van der Pol systems were studied by the multiple scales method and the homotopy analysis method, previously (Qian and Fu 2017, Qian and Zhang 2017, Fu and Qian 2018, Qian *et al.* 2018). Along with the mentioned research studies, the fourth-order Runge–Kutta technique considered in this paper can also be used to solve these equations. Then, the transient vibration of the system is analyzed by performing Hilbert–Huang Transform. In addition, the nonlinear forced vibration characteristics and secondary resonance, in super-harmonic motions, of the system exposed to distributed harmonic load are examined in the form of the frequency response, force response, Poincare map, phase portrait and fast Fourier transforms.

2. Theory of viscoelastically coupled nonlinear models

To get develop the governing equation of motion, the generalized Hamilton's principle is applied (Ajri *et al.* 2018a):

$$\delta\int_{t_1}^{t_2}[U+W-K]dt=0 \tag{1}$$

In which, δ is the variation operator. In addition, T and U are the kinetic energy and elastic strain energy, respectively. Besides, W is viscous dissipation or external forces work. Hence, W can be found as:

$$W=W_{ext}+W_{vis} \tag{2}$$

Inserting Eq. (2) into Eq. (1), and applying the variation operator the Hamilton principle get the following form

$$\int_{t_1}^{t_2}[\delta U+\delta W_{ext}+\delta W_{vis}-\delta K]dt=0 \tag{3}$$

In this paper, the formulation is restricted to small strains, and moderate rotations. Consequently, there is no need to update of the domain, and therefore, the Cauchy and second Piola–Kirchhoff stress tensors are the same. In the MCST proposed by Yang *et al*. (2002), the symmetric part of the curvature tensor χ can obtained from following equation.

$$\chi = \frac{1}{2}(\nabla\omega + (\nabla\omega)^T) \tag{4}$$

In which ω is the rotation vector and can be found from the displacement vector ,u, as following form

$$\omega = \frac{1}{2}\mathrm{curl(u)} \tag{5}$$

Based on the Leaderman constitutive relation (Christensen and Freund 1971), for a viscoelastic nanostructure we have:

$$\begin{gathered} \sigma = \lambda \otimes tr(\varepsilon)I + 2\mu\otimes\varepsilon \\ m = 2l^2\mu\otimes\chi \end{gathered} \tag{6}$$

where m is the couple-stress deviatoric component and σ is the stress tensor. Additionally, λ and μ are time-dependent Lame constants, l is the length-scale parameter of the material and ⊗ is the convolution operator which formulated as

$$g(t)\otimes k(t) = g(0^+)k(t) + \int_{0^+}^{t} \frac{\partial g(t-\tau)}{\partial(t-\tau)}k(\tau)d\tau \tag{7}$$

Eq. (7) is applied to write the constitutive relations as Eq. (8).

$$\begin{aligned} \sigma = \sigma^e + \sigma^v = &\ (\lambda_0 tr(\varepsilon)I + 2\mu_0\varepsilon(t)) \\ &+ \int_0^t (\dot{\lambda}(t-\tau)tr(\varepsilon)I \\ &+ 2\dot{\mu}(t-\tau)\varepsilon(\tau))\,d\tau \end{aligned} \tag{8}$$

$$m = m^e + m^v = 2l^2\mu_0\chi(t) + \int_0^t 2l^2\dot{\mu}(t-\tau)\chi(\tau)d\tau \tag{9}$$

where λ_0 and μ_0 are the Lame constants at the time equal to zero and $\mu(t) = G(t) = E(t)/2(1+\upsilon)$. Moreover, $E(t)$ and $G(t)$ are time-dependent Young's and rigidity modulus and v is the time-independent Poisson ratio. The over dot (·) denotes the first derivation respect to the time.

In order to determine the displacement field of the nanoplate based on the Kirchhoff's plate theory (JE. 1989), the Cartesian coordinate system (x, y, z) with xy-plane is in the mid-plane of the nanoplate, is considered. So we get (Ajri *et al*. 2018a).

$$\begin{gathered} u_x = u(x,y,t) - z\frac{\partial w(x,y,t)}{\partial x} \\ v_y = v(x,y,t) - z\frac{\partial w(x,y,t)}{\partial y} \\ w_z = w(x,y,t) \end{gathered} \tag{10}$$

Considering the von-Karman nonlinearity, the strain components are

$$\begin{gathered} \varepsilon_{xx} = \frac{\partial u}{\partial x} - z\frac{\partial^2 w}{\partial x^2} + \frac{1}{2}\left(\frac{\partial w}{\partial x}\right)^2 \\ \varepsilon_{yy} = \frac{\partial v}{\partial y} - z\frac{\partial^2 w}{\partial y^2} + \frac{1}{2}(\frac{\partial w}{\partial y})^2 \\ \varepsilon_{xy} = \frac{1}{2}\left(\frac{\partial u}{\partial y} + \frac{\partial v}{\partial x} - 2z\frac{\partial^2 w}{\partial x\partial y} + \frac{\partial w}{\partial x}\frac{\partial w}{\partial y}\right) \end{gathered} \tag{11}$$

Substituting Eq. (10) in Eq. (5), result in

$$\omega_x = \frac{\partial w}{\partial y} \qquad \omega_y = -\frac{\partial w}{\partial x} \qquad \omega_z = \frac{1}{2}(\frac{\partial v}{\partial x} - \frac{\partial u}{\partial y}) \tag{12}$$

Also, from Eqs. (4) and (10) can be concluded that

$$\begin{gathered} \chi_{xx} = \frac{\partial^2 w}{\partial x\partial y} \quad \chi_{yy} = -\frac{\partial^2 w}{\partial x\partial y} \\ \chi_{xy} = \frac{1}{2}\left(\frac{\partial^2 w}{\partial y^2} - \frac{\partial^2 w}{\partial x^2}\right) \\ \chi_{xz} = \frac{1}{4}\left(\frac{\partial^2 v}{\partial x^2} - \frac{\partial^2 u}{\partial x\partial y}\right) \quad \chi_{yz} = \frac{1}{4}\left(\frac{\partial^2 v}{\partial x\partial y} - \frac{\partial^2 u}{\partial y^2}\right) \end{gathered} \tag{13}$$

Replacing Eq. (11) into Eq. (8), the following results can be obtained

$$\begin{aligned} \sigma_{xx}^e &= \frac{E_0}{(1-\upsilon^2)}\left[\left(\frac{\partial u}{\partial x} - z\frac{\partial^2 w}{\partial x^2} + \frac{1}{2}\left(\frac{\partial w}{\partial x}\right)^2\right) + \upsilon\left(\frac{\partial v}{\partial y} - z\frac{\partial^2 w}{\partial y^2} + \frac{1}{2}\left(\frac{\partial w}{\partial y}\right)^2\right)\right] \\ \sigma_{xx}^v &= \int_0^t \frac{\dot{E}(t-\tau)}{(1-\upsilon^2)}\left[\left(\frac{\partial u}{\partial x} - z\frac{\partial^2 w}{\partial x^2} + \frac{1}{2}\left(\frac{\partial w}{\partial x}\right)^2\right) + \upsilon\left(\frac{\partial v}{\partial y} - z\frac{\partial^2 w}{\partial y^2} + \frac{1}{2}\left(\frac{\partial w}{\partial y}\right)^2\right)\right]d\tau \\ \sigma_{yy}^e &= \frac{E_0}{(1-\upsilon^2)}\left(\left(\frac{\partial v}{\partial y} - z\frac{\partial^2 w}{\partial y^2} + \frac{1}{2}\left(\frac{\partial w}{\partial y}\right)^2\right) + \upsilon\left(\frac{\partial u}{\partial x} - z\frac{\partial^2 w}{\partial x^2} + \frac{1}{2}\left(\frac{\partial w}{\partial x}\right)^2\right)\right) \\ \sigma_{yy}^v &= \int_0^t \frac{\dot{E}(t-\tau)}{(1-\upsilon^2)}\left[\left(\frac{\partial v}{\partial y} - z\frac{\partial^2 w}{\partial y^2} + \frac{1}{2}\left(\frac{\partial w}{\partial y}\right)^2\right) + \upsilon\left(\frac{\partial u}{\partial x} - z\frac{\partial^2 w}{\partial x^2} + \frac{1}{2}\left(\frac{\partial w}{\partial x}\right)^2\right)\right]d\tau \\ \sigma_{xy}^e &= G_0\left(\frac{\partial u}{\partial y} + \frac{\partial v}{\partial x} - 2z\frac{\partial^2 w}{\partial x\partial y} + \frac{\partial w}{\partial x}\frac{\partial w}{\partial y}\right) \\ \sigma_{xy}^v &= \int_0^t \dot{G}(t-\tau)\left(\frac{\partial u}{\partial y} + \frac{\partial v}{\partial x} - 2z\frac{\partial^2 w}{\partial x\partial y} + \frac{\partial w}{\partial x}\frac{\partial w}{\partial y}\right)d\tau \end{aligned} \tag{14}$$

Similarly, substituting Eq. (13) into Eq. (9), result in following

$$\begin{gathered} m_{xx}^e = 2l^2 G_0\left(\frac{\partial^2 w}{\partial x\partial y}\right) \\ m_{xx}^v = 2l^2\int_0^t \dot{G}(t-\tau)\left(\frac{\partial^2 w}{\partial x\partial y}\right)d\tau \\ m_{yy}^e = -2l^2 G_0\left(\frac{\partial^2 w}{\partial x\partial y}\right) \end{gathered} \tag{15}$$

$$m_{yy}^{v}=-2l^{2}\int_{0}^{t}\dot{G}(t-\tau)\left(\frac{\partial^{2}w}{\partial x\partial y}\right)d\tau$$

$$m_{xy}^{e}=l^{2}G_{0}\left(\frac{\partial^{2}w}{\partial y^{2}}-\frac{\partial^{2}w}{\partial x^{2}}\right)$$

$$m_{xy}^{v}=l^{2}\int_{0}^{t}\dot{G}(t-\tau)\left(\frac{\partial^{2}w}{\partial y^{2}}-\frac{\partial^{2}w}{\partial x^{2}}\right)d\tau$$

$$m_{xz}^{e}=\frac{1}{2}l^{2}G_{0}\left(\frac{\partial^{2}v}{\partial x^{2}}-\frac{\partial^{2}u}{\partial x\partial y}\right)$$

$$m_{xz}^{v}=\frac{1}{2}l^{2}\int_{0}^{t}\dot{G}(t-\tau)\left(\frac{\partial^{2}v}{\partial x^{2}}-\frac{\partial^{2}u}{\partial x\partial y}\right)d\tau$$

$$m_{yz}^{e}=\frac{1}{2}l^{2}G_{0}\left(\frac{\partial^{2}v}{\partial x\partial y}-\frac{\partial^{2}u}{\partial y^{2}}\right)$$

$$m_{yz}^{v}=\frac{1}{2}l^{2}\int_{0}^{t}\dot{G}(t-\tau)\left(\frac{\partial^{2}v}{\partial x\partial y}-\frac{\partial^{2}u}{\partial y^{2}}\right)d\tau$$

Based to the MCST of Yang *et al*. (2002), the first variation of the elastic potential energy is defined as

$$\delta U=\frac{1}{2}\iiint(\sigma^{e}\delta\varepsilon+m^{e}\delta\chi)dv \tag{16}$$

In homogenous rectangular nanoplate the integration respect to volume can be expressed as

$$\int_{V}Fdv=\int_{A}\int_{-h/2}^{h/2}FdzdA \tag{17}$$

Inserting Eq. (17) into Eq. (16) and integrating by parts and after some algebraic processes, the following result is obtained

$$\begin{aligned}\delta U=\int_{A}\Bigg[&-\left(\frac{\partial N_{xx}^{e}}{\partial x}+\frac{\partial N_{xy}^{e}}{\partial y}+\frac{1}{2}\frac{\partial^{2}R_{xz}^{e}}{\partial x\partial y}+\frac{1}{2}\frac{\partial^{2}R_{yz}^{e}}{\partial y^{2}}\right)\partial u\\&-\left(\frac{\partial N_{yy}^{e}}{\partial y}+\frac{\partial N_{xy}^{e}}{\partial x}-\frac{1}{2}\frac{\partial^{2}R_{xz}^{e}}{\partial x^{2}}-\frac{1}{2}\frac{\partial^{2}R_{yz}^{e}}{\partial x\partial y}\right)\partial v\\&-\left(\frac{\partial^{2}M_{xx}^{e}}{\partial x^{2}}+\frac{\partial^{2}M_{yy}^{e}}{\partial y^{2}}+2\frac{\partial^{2}M_{xy}^{e}}{\partial x\partial y}-\frac{\partial^{2}R_{xx}^{e}}{\partial x\partial y}-\frac{\partial^{2}R_{xy}^{e}}{\partial y^{2}}+\frac{\partial^{2}R_{xy}^{e}}{\partial x^{2}}+\frac{\partial^{2}R_{yy}^{e}}{\partial x\partial y}+P^{e}(w)\right)\partial w\Bigg]dA\end{aligned} \tag{18}$$

where

$$N_{ij}^{e}=\int_{-h/2}^{h/2}\sigma_{ij}^{e}dz\quad M_{ij}^{e}=\int_{-h/2}^{h/2}z\sigma_{ij}^{e}dz\quad R_{ij}^{e}=\int_{-h/2}^{h/2}m_{ij}^{e}dz \tag{19}$$

and

$$P^{e}(w)=\frac{\partial}{\partial x}\left(N_{xx}^{e}\frac{\partial w}{\partial x}+N_{xy}^{e}\frac{\partial w}{\partial y}\right)+\frac{\partial}{\partial y}\left(N_{xy}^{e}\frac{\partial w}{\partial x}+N_{yy}^{e}\frac{\partial w}{\partial y}\right) \tag{20}$$

Similarly, the viscous forces virtual work first variation on the nanoplate is givens as

$$\delta W_{vis}=\delta U_{vis}=\frac{1}{2}\iiint(\sigma^{v}\delta\varepsilon+\mathrm{m}^{v}\delta\chi)dv \tag{21}$$

By integration, we get:

$$\begin{aligned}\delta U_{vis}=\int_{A}\Bigg[&-\left(\frac{\partial N_{xx}^{v}}{\partial x}+\frac{\partial N_{xy}^{v}}{\partial y}+\frac{1}{2}\frac{\partial^{2}R_{xz}^{v}}{\partial x\partial y}+\frac{1}{2}\frac{\partial^{2}R_{yz}^{v}}{\partial y^{2}}\right)\partial u\\&-\left(\frac{\partial N_{yy}^{v}}{\partial y}+\frac{\partial N_{xy}^{v}}{\partial x}-\frac{1}{2}\frac{\partial^{2}R_{xz}^{v}}{\partial x^{2}}-\frac{1}{2}\frac{\partial^{2}R_{yz}^{v}}{\partial x\partial y}\right)\partial v\\&-\left(\frac{\partial^{2}M_{xx}^{v}}{\partial x^{2}}+\frac{\partial^{2}M_{yy}^{v}}{\partial y^{2}}+2\frac{\partial^{2}M_{xy}^{v}}{\partial x\partial y}-\frac{\partial^{2}R_{xx}^{v}}{\partial x\partial y}-\frac{\partial^{2}R_{xy}^{v}}{\partial y^{2}}+\frac{\partial^{2}R_{xy}^{v}}{\partial x^{2}}+\frac{\partial^{2}R_{yy}^{v}}{\partial x\partial y}+P^{v}(w)\right)\partial w\Bigg]dA\end{aligned} \tag{22}$$

where

$$N_{ij}^{v}=\int_{-h/2}^{h/2}\sigma_{ij}^{v}dz\quad M_{ij}^{v}=\int_{-h/2}^{h/2}z\sigma_{ij}^{v}dz\quad R_{ij}^{v}=\int_{-h/2}^{h/2}m_{ij}^{v}dz \tag{23}$$

and

$$P^{v}(w)=\frac{\partial}{\partial x}\left(N_{xx}^{v}\frac{\partial w}{\partial x}+N_{xy}^{v}\frac{\partial w}{\partial y}\right)+\frac{\partial}{\partial y}\left(N_{xy}^{v}\frac{\partial w}{\partial x}+N_{yy}^{v}\frac{\partial w}{\partial y}\right) \tag{24}$$

From the general expression of the external forces work in the MCST, the virtual work first variation performed by the applied forces on the viscoelastic nanoplate in the time interval [0, T] can be calculated as (Mockensturm and Guo 2005)

$$\begin{aligned}\delta W_{ext}=&-\int_{\Gamma}\left(t_{x}\delta u+t_{y}\delta v+t_{z}\delta w+s_{x}\delta\omega_{1}+s_{y}\delta\omega_{2}+s_{z}\delta\omega_{3}\right)d\Gamma\\&-\int_{\Omega}\left((f_{x}+q_{x})\delta u+(f_{y}+q_{y})\delta v+(f_{z}+q_{z})\delta w+c_{x}\delta\omega_{1}+c_{y}\delta\omega_{2}+c_{z}\delta\omega_{3}\right)dA\end{aligned} \tag{25}$$

where Ω and Γ are, respectively, the nanoplate middle surface and the middle surface boundary (Ma *et al.* 2011, Reddy and Kim 2012), (f_x ,f_y ,f_z) and the(c_x ,c_y ,c_z) are, respectively, the body forces and the body couples, and (q_x ,q_y ,q_z), (t_x ,t_y ,t_z) and (s_x ,s_y ,s_z) are, respectively, the tractions applied on Γ, the surface couple and Cauchy traction applied on S (Ajri *et al.* 2018a).

The kinetic energy first variation is given as

$$\delta \mathrm{K}=\int \rho[\dot{u}_x \delta \dot{u}_x+\dot{v}_y \delta \dot{u}_y+\dot{w}_z \delta \dot{w}_z] dV \tag{26}$$

where ρ is the nanoplate mass density.

By applying the time first derivative for Eq. (10) and substituting in Eq. (26) we get:

$$\begin{aligned}\delta \mathrm{K}=\int_A \Big\{ & I_0(\dot{u}\delta\dot{u}+\dot{v}\delta\dot{v}+\dot{w}\delta\dot{w}) \\ & +I_2\left(\frac{\partial\dot{w}}{\partial x}.\frac{\partial\delta\dot{w}}{\partial x}+\frac{\partial\dot{w}}{\partial y}.\frac{\partial\delta\dot{w}}{\partial y}\right) \\ & -I_1\left(\dot{u}\frac{\partial\delta\dot{w}}{\partial x}+\delta\dot{u}\frac{\partial\dot{w}}{\partial x}+\dot{v}\frac{\partial\delta\dot{w}}{\partial y} \right. \\ & \left.\left. +\delta\dot{v}\frac{\partial\dot{w}}{\partial y}\right)\right\} dA\end{aligned} \tag{27}$$

where

$$\int_{-h/2}^{h/2}(1,z,z^2)\rho dz=(I_0,I_1,I_2) \tag{28}$$

By replacing the exprressions for δU, δW_{vis}, δW_{ext} and δK from the Eq.(18), (22), (25) and (27) into Eq. (3) and applying the partial integration method, the governing motion equations for viscoelastic nanoplate on the basis of the MCS theory can be obtained as Eq. (29)

$$\begin{aligned}\delta u:\ & \frac{\partial N_{xx}}{\partial x}+\frac{\partial N_{xy}}{\partial y}+\frac{1}{2}\left(\frac{\partial^2 R_{xz}}{\partial x\partial y}+\frac{\partial^2 R_{yz}}{\partial y^2}\right)+f_x+q_x \\ & +\frac{1}{2}\frac{\partial c_z}{\partial y}=I_0\ddot{u}-I_1\frac{\partial\ddot{w}}{\partial x} \\ \delta v:\ & \frac{\partial N_{yy}}{\partial y}+\frac{\partial N_{xy}}{\partial x}-\frac{1}{2}\left(\frac{\partial^2 R_{xz}}{\partial x^2}+\frac{\partial^2 R_{yz}}{\partial x\partial y}\right)+f_y+q_y \\ & -\frac{1}{2}\frac{\partial c_z}{\partial y}=I_0\ddot{v}-I_1\frac{\partial\ddot{w}}{\partial y} \\ \delta w:\ & \frac{\partial^2 M_{xx}}{\partial x^2}+\frac{\partial^2 M_{yy}}{\partial y^2}+2\frac{\partial^2 M_{xy}}{\partial x\partial y} \\ & +\frac{\partial^2(R_{yy}-R_{xx})}{\partial x\partial y}+R_{xy}\left(\frac{\partial^2}{\partial x^2}-\frac{\partial^2}{\partial y^2}\right)+P(w) \\ & +f_z+q_z-\frac{\partial c_x}{\partial y}+\frac{\partial c_y}{\partial x} \\ & =I_0\ddot{w}-I_2\left(\frac{\partial^2\ddot{w}}{\partial x^2}+\frac{\partial^2\ddot{w}}{\partial y^2}\right)+I_1\left(\frac{\partial\ddot{u}}{\partial x}+\frac{\partial\ddot{v}}{\partial y}\right)\end{aligned} \tag{29}$$

where $N_{ij}=N_{ij}^e+N_{ij}^v$, $M_{ij}=M_{ij}^e+M_{ij}^v$ and $P=P^e+P^v$.Equation (29) contains the set of nonlinear integral-differential equations for a viscoelastic nano-resonator in the framework of the MCST. In the current model, the length-scale parameter presents in current and past history terms and affects both of them. Additionally, with removing the past-history terms in Eq.(29), one can reach the governing equations of the elastic nano-resonator. This gives us the correctness of our calculations in obtaining governing equations.

The displacement form of Eq.(29) can be written as.

$$\begin{aligned}\delta u:\ & \frac{E_0 h}{(1-\upsilon^2)}\left(\frac{\partial^2 u}{\partial x^2}+\frac{\partial w}{\partial x}\frac{\partial^2 w}{\partial x^2}\right. \\ & \left.+\upsilon\left(\frac{\partial^2 v}{\partial x\partial y}+\frac{\partial w}{\partial y}\frac{\partial^2 w}{\partial x\partial y}\right)\right) \\ & +\int_0^t \frac{h\dot{E}(t-\tau)}{(1-\upsilon^2)}\left(\frac{\partial^2 u}{\partial x^2}+\frac{\partial w}{\partial x}\frac{\partial^2 w}{\partial x^2}\right. \\ & \left.+\upsilon\left(\frac{\partial^2 v}{\partial x\partial y}+\frac{\partial w}{\partial y}\frac{\partial^2 w}{\partial x\partial y}\right)\right)d\tau \\ & +G_0 h\left(\frac{\partial^2 u}{\partial y^2}+\frac{\partial^2 v}{\partial x\partial y}+\frac{\partial w}{\partial x}\frac{\partial^2 w}{\partial y^2}\right. \\ & \left.+\frac{\partial^2 w}{\partial x\partial y}\frac{\partial w}{\partial y}\right) \\ & +\int_0^t h\dot{G}(t-\tau)\left(\frac{\partial^2 u}{\partial y^2}+\frac{\partial^2 v}{\partial x\partial y}\right. \\ & \left.+\frac{\partial w}{\partial x}\frac{\partial^2 w}{\partial y^2}+\frac{\partial^2 w}{\partial x\partial y}\frac{\partial w}{\partial y}\right)d\tau \\ & +\frac{l^2 h}{4}G_0\left(\frac{\partial^4 v}{\partial x^3\partial y}-\frac{\partial^4 u}{\partial x^2\partial y^2}\right) \\ & +\frac{l^2 h}{4}\int_0^t \dot{G}(t-\tau)\left(\frac{\partial^4 v}{\partial x^3\partial y}\right. \\ & \left.-\frac{\partial^4 u}{\partial x^2\partial y^2}\right)d\tau \\ & +\frac{l^2 h}{4}G_0\left(\frac{\partial^4 v}{\partial x\partial y^3}-\frac{\partial^4 u}{\partial y^4}\right) \\ & +\frac{l^2 h}{4}\int_0^t \dot{G}(t-\tau)\left(\frac{\partial^4 v}{\partial x\partial y^3}\right. \\ & \left.-\frac{\partial^4 u}{\partial y^4}\right)d\tau+f_x+q_x+\frac{1}{2}\frac{\partial c_z}{\partial y} \\ & -I_0\ddot{u}+I_1\frac{\partial\ddot{w}}{\partial x}=0\end{aligned} \tag{30-a}$$

$$\begin{aligned}\delta v:\ & \frac{E_0 h}{(1-\upsilon^2)}\left(\frac{\partial^2 v}{\partial y^2}+\frac{\partial w}{\partial y}\frac{\partial^2 w}{\partial y^2}\right. \\ & \left.+\upsilon\left(\frac{\partial^2 u}{\partial x\partial y}+\frac{\partial w}{\partial x}\frac{\partial^2 w}{\partial x\partial y}\right)\right)\end{aligned} \tag{30-b}$$

$$+\int_0^t \frac{h\dot{E}(t-\tau)}{(1-\upsilon^2)}\left(\frac{\partial^2 v}{\partial y^2}+\frac{\partial w}{\partial y}\frac{\partial^2 w}{\partial y^2}+\upsilon\left(\frac{\partial^2 u}{\partial x\partial y}+\frac{\partial w}{\partial x}\frac{\partial^2 w}{\partial x\partial y}\right)\right)d\tau+G_0 h\left(\frac{\partial^2 v}{\partial x^2}+\frac{\partial^2 u}{\partial x\partial y}+\frac{\partial w}{\partial y}\frac{\partial^2 w}{\partial x^2}+\frac{\partial^2 w}{\partial x\partial y}\frac{\partial w}{\partial x}\right)$$
$$+\int_0^t h\dot{G}(t-\tau)\left(\frac{\partial^2 v}{\partial x^2}+\frac{\partial^2 u}{\partial x\partial y}+\frac{\partial w}{\partial y}\frac{\partial^2 w}{\partial x^2}+\frac{\partial^2 w}{\partial x\partial y}\frac{\partial w}{\partial x}\right)d\tau+\frac{l^2 h}{4}G_0\left(\frac{\partial^4 u}{\partial y^3\partial x}-\frac{\partial^4 v}{\partial x^2\partial y^2}\right)+\frac{l^2 h}{4}\int_0^t \dot{G}(t-\tau)\left(\frac{\partial^4 u}{\partial y^3\partial x}-\frac{\partial^4 v}{\partial x^2\partial y^2}\right)d\tau+\frac{l^2 h}{4}G_0\left(\frac{\partial^4 u}{\partial y\partial x^3}-\frac{\partial^4 v}{\partial x^4}\right)+\frac{l^2 h}{4}\int_0^t \dot{G}(t-\tau)\left(\frac{\partial^4 u}{\partial y\partial x^3}-\frac{\partial^4 v}{\partial x^4}\right)d\tau+f_y+q_y-\frac{1}{2}\frac{\partial c_z}{\partial x}-I_0\ddot{v}+I_1\frac{\partial \ddot{w}}{\partial y}=0$$

$$\delta w:\ -\left(\frac{h^3}{12(1-\upsilon^2)}+\frac{hl^2}{2(1+\upsilon)}\right)\left(E_0\nabla^4 w+\int_0^t \dot{E}(t-\tau)\,\nabla^4 w(\tau)d\tau\right)+\frac{h}{1-\upsilon^2}\left(E_0 \mathrm{P}(w)+\int_0^t \dot{E}(t-\tau)\,\mathrm{P}(w(\tau))d\tau\right)+\mathrm{f}_z+q_z-\frac{\partial c_x}{\partial y}+\frac{\partial c_y}{\partial x}-I_0\ddot{w}+I_2\left(\frac{\partial^2 \ddot{w}}{\partial y^2}+\frac{\partial^2 \ddot{w}}{\partial x^2}\right)-I_1\left(\frac{\partial \ddot{u}}{\partial x}+\frac{\partial \ddot{v}}{\partial y}\right)=0 \tag{30-c}$$

where

$$P(w)=\frac{h}{1-\upsilon^2}\left[\frac{\partial^2 w}{\partial x^2}\left(\frac{\partial u}{\partial x}+\frac{1}{2}\frac{\partial w}{\partial x}\frac{\partial w}{\partial x}+\upsilon\frac{\partial v}{\partial y}+\frac{\upsilon}{2}\frac{\partial w}{\partial y}\frac{\partial w}{\partial y}\right)+\frac{\partial^2 w}{\partial y^2}\left(\frac{\partial v}{\partial y}+\frac{1}{2}\frac{\partial w}{\partial y}\frac{\partial w}{\partial y}+\upsilon\frac{\partial u}{\partial x}+\frac{\upsilon}{2}\frac{\partial w}{\partial x}\frac{\partial w}{\partial x}\right)+(1-\upsilon)\frac{\partial^2 w}{\partial x\partial y}\left(\frac{\partial u}{\partial y}+\frac{\partial v}{\partial x}+\frac{\partial w}{\partial x}\frac{\partial w}{\partial y}\right)\right] \tag{31}$$

For homogenous rectangular plate, I_1 become zero.

The following nondimensional variables are introduced:

$$\bar{w}=\frac{w}{h}\quad \bar{x}=\frac{x}{a}\quad \bar{y}=\frac{y}{b}\quad \xi=\frac{a}{b}\quad l_0=\frac{l}{h}\quad \bar{f}=\frac{\mathrm{f}_z a^4}{E_0 h^4}$$
$$\bar{t}=\frac{t}{T}\quad \mathrm{T}=\sqrt{\frac{I_0 a^4}{E_0 h^3}} \tag{32}$$

where a, b and h are the nanoplate length, width and thickness, respectively.

Based on the experimental results on the viscoelastic material (Lee *et al.* 2005, Yan *et al.* 2009), the standard anelastic solid model is applied to express the relaxation function. Then we get (Ajri *et al.* 2018a)

$$E(t)=C+De^{-\gamma t} \tag{33}$$

In which γ is the relaxation coefficient. Besides, the $E(t{=}0)$ represents the initial elastic modulus E_0

$$n(t)=\frac{E(t)}{E_0}=\bar{C}+\bar{D}e^{-\bar{\gamma}t} \tag{34}$$

where $\bar{C}=\frac{C}{C+D}$ $\bar{D}=\frac{D}{C+D}$ and $\bar{\gamma}=\gamma T$

The present study considers the rectangular nanoplate with all edges simply supported. The solutions are assumed as (Niyogi 1973).

$$u(\bar{x},\bar{y},\bar{t})=\frac{1}{16}\sum_{m=1}^{\infty}\sum_{n=1}^{\infty}\alpha\frac{h}{a}\Phi^2{}_{mn}(\bar{t})sin2\alpha\bar{x}\left(cos2\beta\bar{y}-1+\upsilon\xi^2\left(\frac{\beta}{\alpha}\right)^2\right)$$
$$v(\bar{x},\bar{y},\bar{t})=\frac{1}{16}\sum_{m=1}^{\infty}\sum_{n=1}^{\infty}\beta\frac{h}{b}\Phi^2{}_{mn}(\bar{t})sin2\beta\bar{y}\left(cos2\alpha\bar{x}-1+\upsilon\frac{1}{\xi^2}\left(\frac{\alpha}{\beta}\right)^2\right) \tag{35}$$
$$w(\bar{x},\bar{y},\bar{t})=\sum_{m=1}^{\infty}\sum_{n=1}^{\infty}\Phi_{mn}(\bar{t})sin\alpha\bar{x}sin\beta\bar{y}$$

where α=mπ and β=nπ.

In this research, only the harmonic transverse force, f cosΩt, is assumed to be applied on the nano-resonator. Similarly, the out of plane load amplitude $\bar{f}$ can be expanded in the double-Fourier sine series

$$\bar{f}(\bar{x},\bar{y}) = \sum_{m=1}^{\infty}\sum_{n=1}^{\infty} f\, sin\alpha\bar{x}sin\beta\bar{y} \tag{36}$$

where

$$f = 4\int_0^1\int_0^1 \bar{f}(\bar{x},\bar{y})sin\alpha\bar{x}sin\beta\bar{y}d\bar{x}d\bar{y} \tag{37}$$

To solve the Eq. 30(c) for $\Phi_{mn}(t)$**,** the Bubnov–Galerkin approach is applied, (Ajri *et al.* 2018a) and the following integral is computed (with dropping the asterisk notation for brevity).

$$\int_0^1\int_0^1 \Lambda sin\alpha x sin\beta y\, dxdy = 0 \tag{38}$$

where Λ is the left-hand side of the Eq. 30(c). Replacing Eq. (35) into Eq.30(c), the following expression of Λ can be obtained:

$$\Lambda = \left\{\frac{-1}{16(1-\upsilon^2)}\left(4\upsilon\xi^2\alpha^2\beta^2 + 2(\alpha^4+\xi^4\beta^4) + 2(\upsilon^2-1)(\alpha^4cos2\beta y + \xi^4\beta^4cos2\alpha x)\right) \times\left(\Phi^3(t) - D\gamma\int_0^t e^{-\gamma(t-\tau)}\,\Phi^3(\tau)d\tau\right) + fcos\Omega t - \left(\frac{1}{12(1-\upsilon^2)} + \frac{1}{2(1+\upsilon)}l_0^2\right)(\alpha^2+\xi^2\beta^2)^2\left(\Phi(t) - D\gamma\int_0^t e^{-\gamma(t-\tau)}\,\Phi(\tau)d\tau\right) - \ddot{\Phi}\right\} sin\alpha x\; sin\beta y \tag{39}$$

Using Bubnov–Galerkin approach and setting the integral to zero, the solution of $\Phi_{mn}(t)$ is obtained as Eq. (40)

$$\frac{1}{16(1-\upsilon^2)}\left(4\upsilon\xi^2\alpha^2\beta^2 + (3-\upsilon^2)(\alpha^4+\xi^4\beta^4)\right)\left(\Phi^3(t) - D\gamma\int_0^t e^{-\gamma(t-\tau)}\,\Phi^3(\tau)d\tau\right) + \left(\frac{1}{12(1-\upsilon^2)} + \frac{1}{2(1+\upsilon)}l_0^2\right)(\alpha^2+\xi^2\beta^2)^2\left(\Phi(t) - D\gamma\int_0^t e^{-\gamma(t-\tau)}\,\Phi(\tau)d\tau\right) + \ddot{\Phi}(t) = fcos\Omega t \tag{40}$$

The Eq. (40) is a nonlinear integro-differential equation for plate-shape nano-resonator using Leaderman viscoelastic model and the MCST. After some algebraic processes, the fourth order Runge-Kutta method is used to solve this equation (Fu and Zhang 2009).

3. Results for viscoelastically coupled size-dependent dynamics

In this section, the numerical results are presented. The nano-resonator is supposed to be made of epoxy with the following geometric and mechanical properties: $\xi = 2$, $E = 1.44$ GPa, $\rho = 1120$ kg/m^3, $\upsilon = 0.38$ and $\bar{C} = 0.7$ $\bar{D} = 0.3$

3.1 Free vibration

In nonlinear nanosystem the vibration amplitude alter the natural frequencies. The existence of the integral terms in Eq.(40) achieved from the Leadermen viscoelastic model cause to decrease the motion amplitude over the time.Consequently, the nonlinearity effects decrease and the nanosystem frequencies varies with the time. In order to evaluate the viscoelastic nanosystem natural frequencies, the Hilbert–Huang transform (HHT) are performed. (Huang *et al.* 1998, Huang *et al.* 1999)

The dimensionless natural frequency over time for elastic ($\gamma = 0$) and viscoelastic nanosystems with $\gamma = 1$ and $\gamma = 3$ obtained by the HHT and displayed in Fig. 1 for three different initial condition values $\dot{\Phi}_0$=100, 50 and 10. The thickness ratio is selected as *h/l*=1. Obviously, it is seen that in the elastic nanosystem, $\gamma = 0$, the frequencies remain constant over the time at each excitation value. Therefore, the elastic model vibration is stationary. Additionally, the higher natural frequencies predicted at bigger initial condition (33.3, 39.5 and 50.2 for $\dot{\Phi}_0$=10, 50 and 100, respectively). However, the viscoelastic model behavior is different over the time for the selected initial condition. The Fig. 1(c) demonstrates that at $\dot{\Phi}_0$=10 the natural frequency of the viscoelastic model similar to the elastic remain constant over the time. This happens since the nanosystem has weaker nonlinearity at the smaller motion amplitudes. However, at $\dot{\Phi}_0$=50 and 100 the non-dimensional frequencies of the viscoelastic model decrease form 39.5 and 50.2 at initial time (*t*=0) to 33.9 and 34.5 at *t*=9. This is due to decreasing the vibration amplitude and nonlinearity effects over the time for the viscoelastic model. Furthermore, it is observed that the viscoelastic model frequencies are smaller than the elastic ones.

Fig. 2 displays the variation of natural frequencies for the transverse motion vs. the thickness ratios (*h/l*) in the

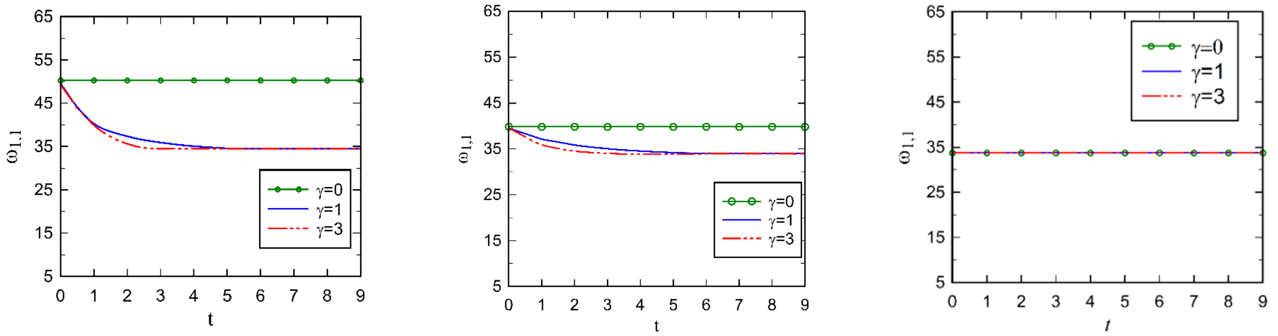

(a) (b) (c)

Fig. 1 Natural frequency variation over time based on HHT method: (a–c) for initial excitation value $\dot{\Phi}_0$=100, 50 and 10, respectively)

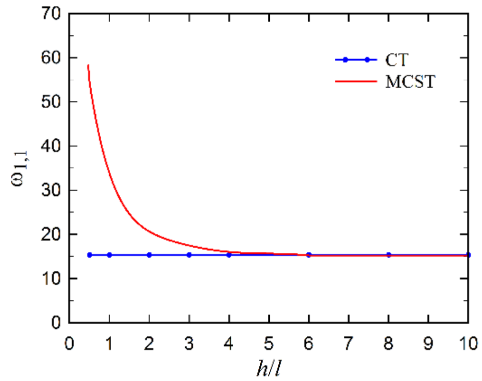

Fig. 2 Transverse motion dimensionless fundamental frequency thickness ratio

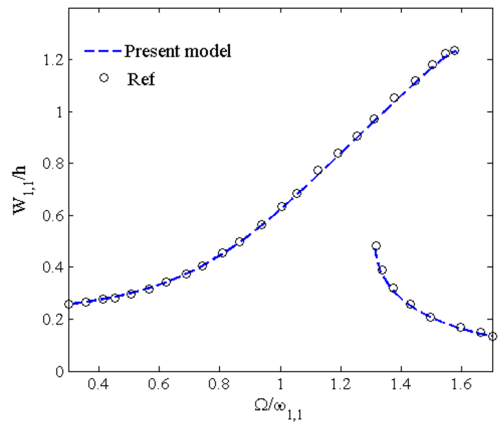

Fig. 3 The frequency response of the out-of-plane motion for l=0: dashed line and unfilled circle predicted by current study and Amabili (2004), respectively

framework of the viscoelastic MCST and classical theory (for $\gamma = 1$ and $\dot{\Phi}_0$ =10). This figure shows that the predicted fundamental natural frequencies by the proposed model are larger than the size-independent classical theory at each thickness ratio. Therefore, the size-dependent MCST-based model increases the nano-resonator stiffness. Furthermore, the curves trend show that the differences in fundamental frequencies predicted by these two models are larger at thickness ratios smaller than 3, while they decrease with increasing the thickness ratios. Consequently, at smaller thickness ratios, the size effect becomes prominent.

3.2 Dynamic analysis

The nanosystem nonlinear dynamic is discussed in this section by plotting the frequency and force response, Poincare map, phase portrait and fast Fourier transforms. For this purpose, the effects of thickness ratios and applied force amplitudes on the dynamic responses of the nanosystem are examined. Moreover, the differences in the dynamic response of the nanosystem with and without the small-scale effects are inspected in order to illustrate the importance of using the MCS theory respect to the size-independent CT. It is worth noting that in this section the stable solution obtained from the forward numerical method, the forth order Rung-Kutta technique, is provided.

Before presentation of the dynamic results, in order to validate the model and applied solution approached of the governing equations, a comparative diagram is shown in Fig. 3. In this figure, the out-of-plane motion frequency response predicted by the current model for l=0 is plotted and compared with the same results obtained by Amabili (2004). It can be seen that the results are close to each other.

Fig. 4 shows the frequency response curves, maximum amplitude versus excitation frequency, of the nanosystem for h/l= 1, 5, 10 and 20, respectively. The dimensionless relaxation coefficient, initial excitation value and the distributed transverse force amplitude values are assumed as γ=3, $\dot{\Phi}_0$=10 and f=10. The excitation force frequency is normalized by the nonlinear fundamental natural frequencies. This figure displays that the nanosystem under consideration has hardening type dynamic behavior. According to the results, with increasing the thickness ratio of the nanosystem the hardening behavior becomes stronger. Moreover, the figure reveals that there are two saddle-node bifurcations that happen in Ω= 1.134 $\omega_{1,1}$ and Ω=1.157$\omega_{1,1}$ for h/l=10 and Ω=1.13 $\omega_{1,1}$ and Ω= 1.15 $\omega_{1,1}$ for h/l=20.

The effects of the applied force amplitude on the frequency response of the nanosystem emphasized in Fig. 5(a–d). The dimensionless relaxation coefficient and thickness ratios are selected γ=3 and h/l=1,5. The figures show that there is no extra peak in the frequency response

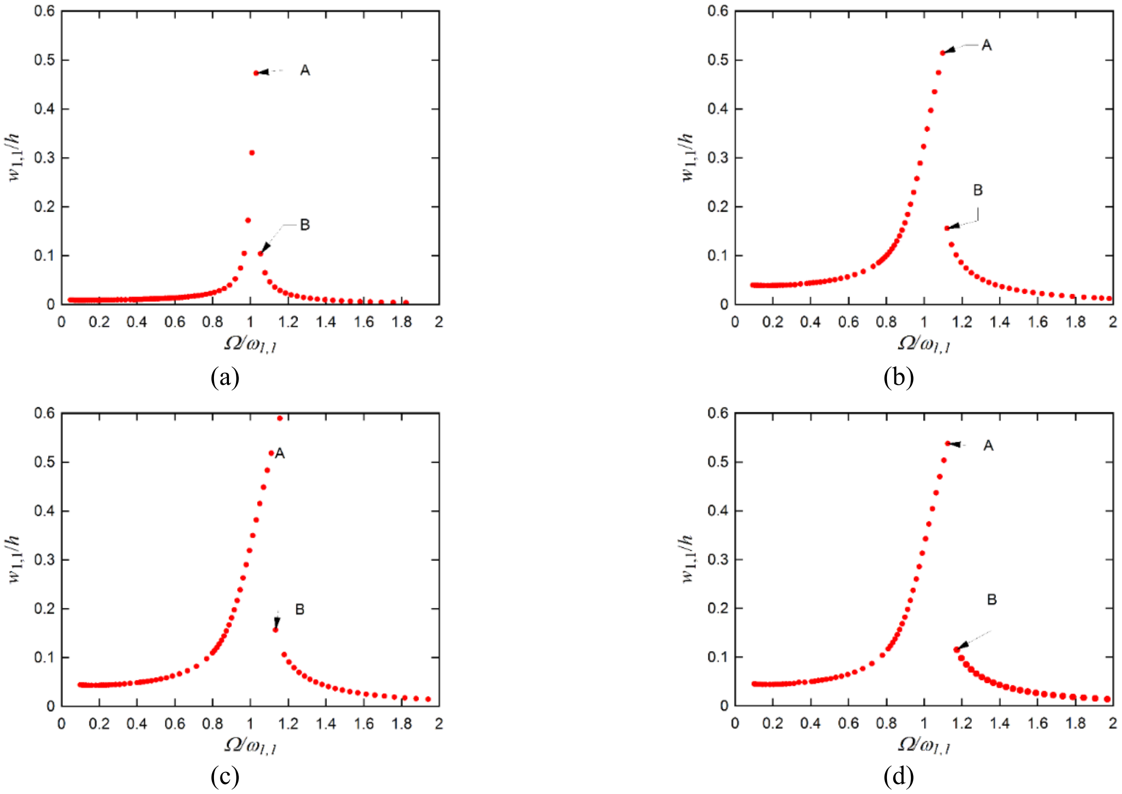

Fig. 4 The *h/l* effects on the frequency response of the nonlinear viscoelastic nanosystem: (a–d) the maximum amplitudes for *h/l*=1, 5, 10 and 20, respectively

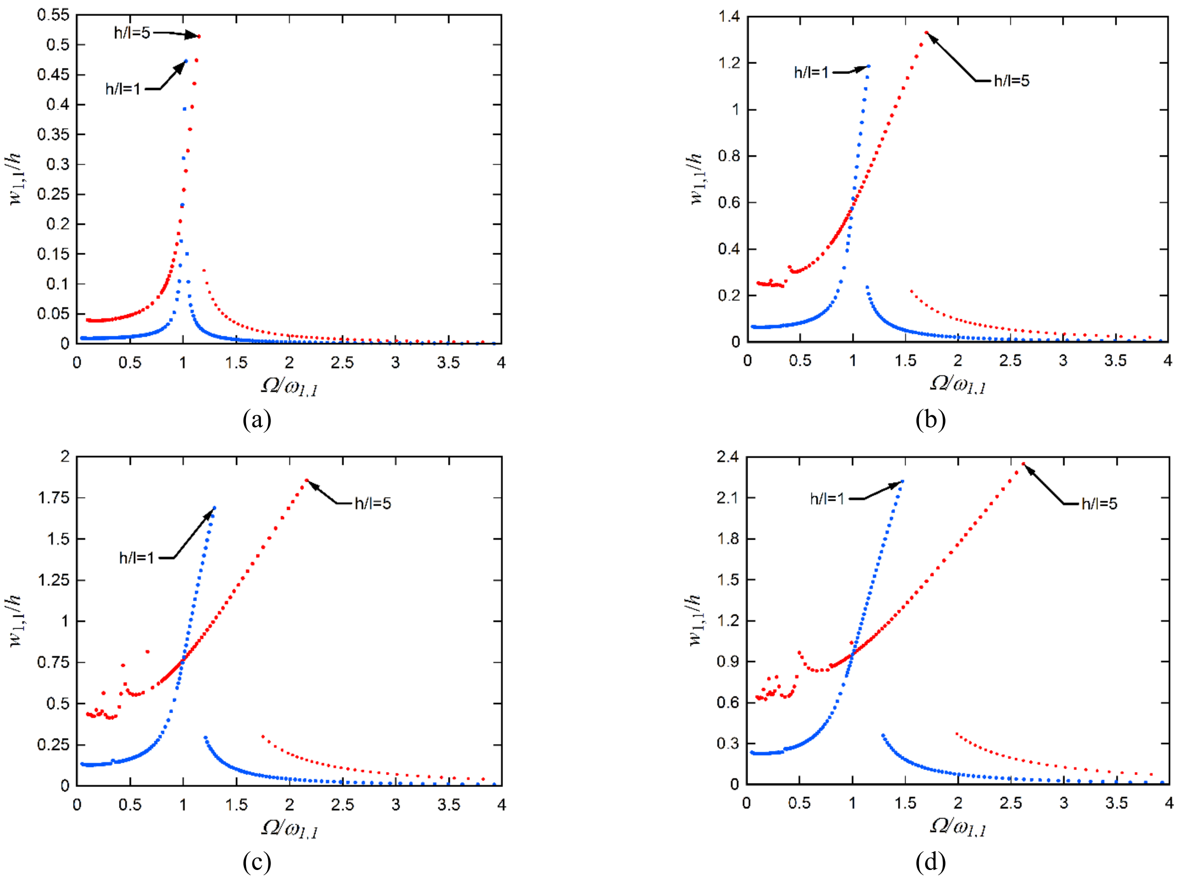

Fig. 5 The applied force amplitude effects on the frequency response of the nonlinear viscoelastic nanosystem: (a–d) the maximum amplitudes for *f*=10, 70,140 and 250 respectively

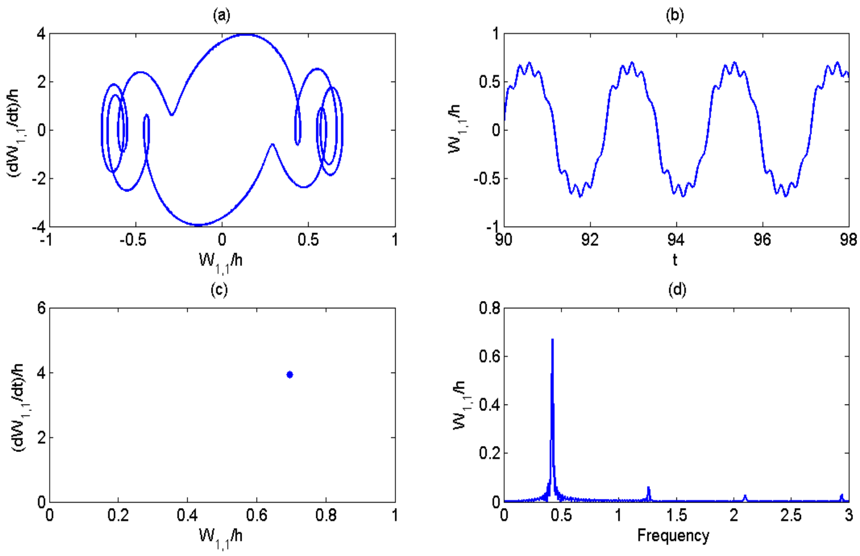

Fig. 6 Phase plane,time history, Poincare map and Frequency spectrum of the nanosystem at Ω= 0.167$\omega_{1,1}$ with *h/l*=5 and *f*=250

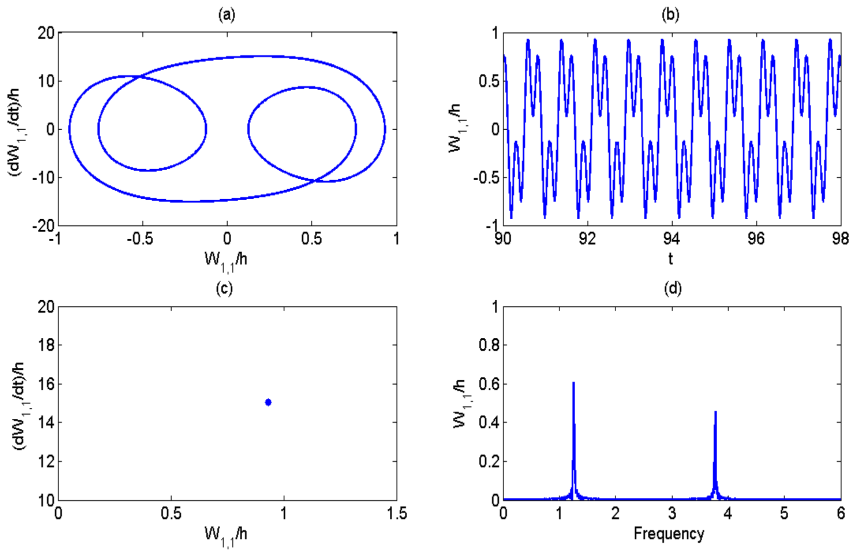

Fig. 7 Phase plane, time history, Poincare map and Frequency spectrum of the nanosystem, respectively at Ω= 0.5$\omega_{1,1}$ with *h/l*=5 and *f*=250

of the nanosystem with thickness ratio equaling to 1. However, the Fig. 5(b)reveals that there are two extra peaks before the resonance peak of the nanosystem with *h/l*=5 in the neighborhood of Ω = 0.22$\omega_{1,1}$ and Ω = 0.39$\omega_{1,1}$. In addition, Fig. 5(c-d) depicts that at the higher forcing amplitudes, the number of the secondary resonances increases and their amplitudes become bigger. The weaker hardening type behaviors are also seen in the secondary resonances. Moreover, the saddle-node bifurcations are shifted to higher frequency ratios at the bigger forcing amplitudes.

In order to scrutinize the dynamic response more, the Phase plane, time history response, Poincare map and the frequency spectrum, using the Fast Fourier Transform, of the nanosystem at different frequency ratios, *f*=250 and *h/l*=5, are depicted in Figs. 6-8. The figures are plotted for Ω= 0.167$\omega_{1,1}$, Ω=0.5$\omega_{1,1}$ and Ω=1.62$\omega_{1,1}$. The frequency spectrum shows that the nanosystem has super-harmonic motion at Ω= 0.167$\omega_{1,1}$ and the Fast Fourier Transform, FFT, shows that there are several peaks in the frequnecies equaling to 0.42,1.25, 2.1 and 2.94. Similarly, Fig. 7 shows the existance of the super-harmonic motion at Ω= 0.5$\omega_{1,1}$ and the two peaks are seen in the frequencies equaling to 1.25 and 3.77 in FFT analysis. This is the reason why the extra peaks are seen at these frequency ratios in Fig. 5(d).

Also, Fig. 8 demonstrates that at Ω=1.62$\omega_{1,1}$ the phase planes create a continuous and closed curve and the Poincare maps create one point. Therefore, the nanosystem has a periodic motion at this frequency ratio.

The effects of the external force amplitude on the vibration amplitude of the nanosystem of Fig. 4 at different normalized frequencies, Ω/ $\omega_{1,1}$=0.99,1, 1.02 and 1.03, are

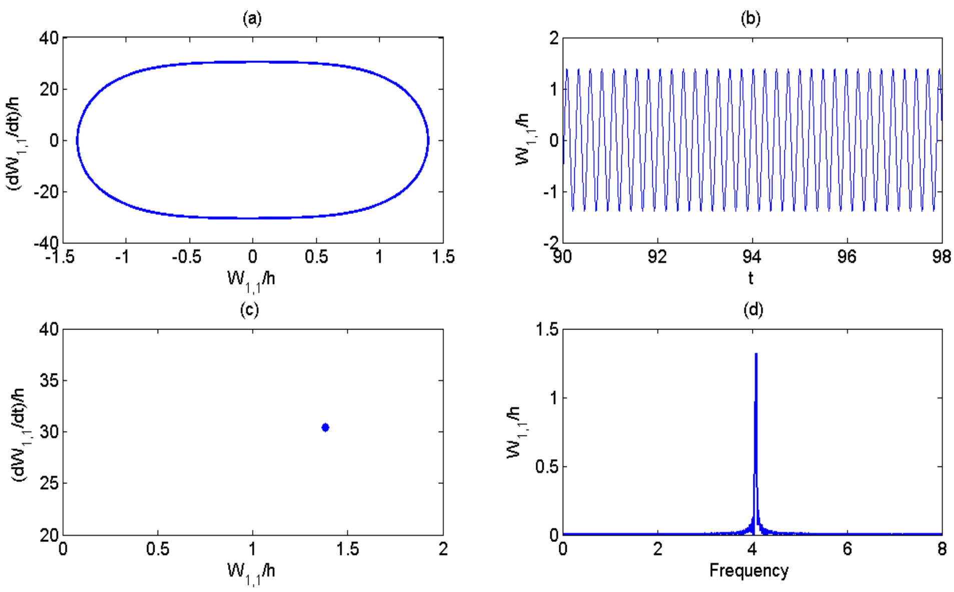

Fig. 8 Phase plane, time history, Poincare map and frequency spectrum of the nanosystem, respectively at Ω= 1.62 $\omega_{1,1}$ with *h/l*=5 and *f*=250

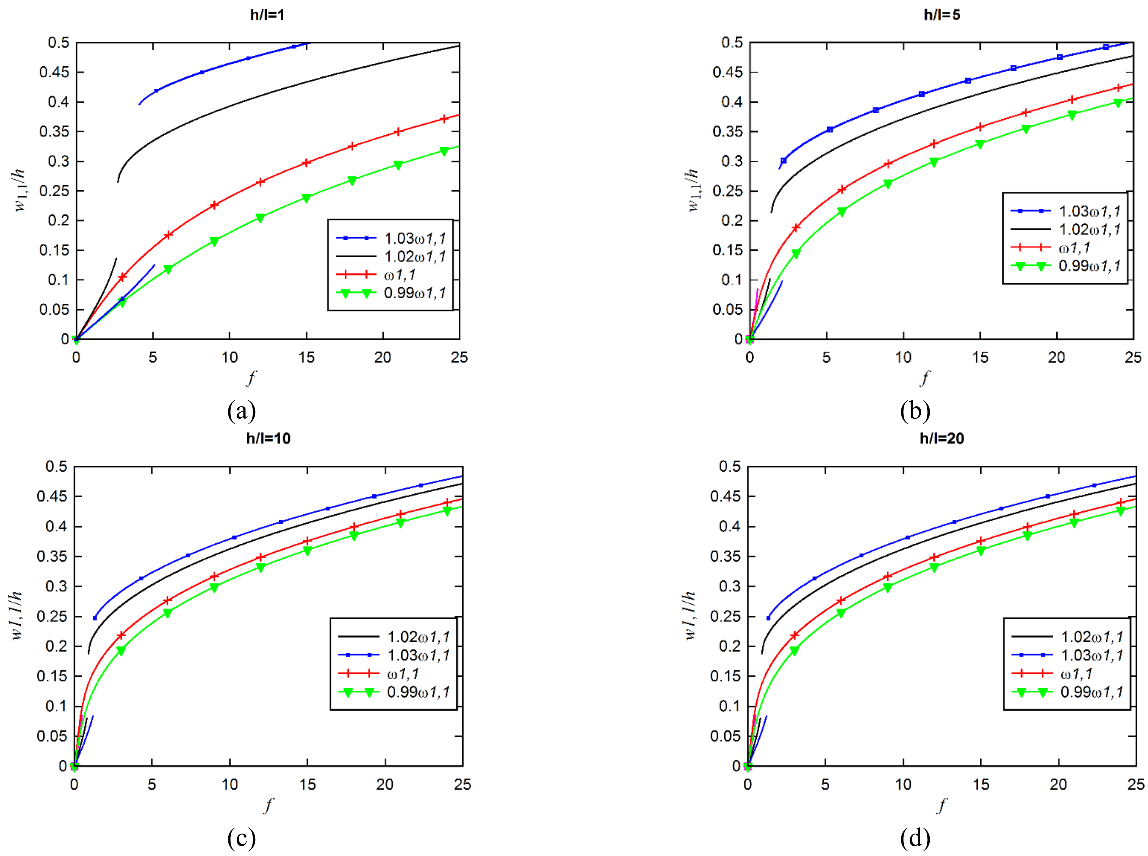

Fig. 9 The nanosystem force response at four frequency ratios ($\Omega/\ \omega_{1,1}$ = 0.99, 1, 1.02, 1.03) at different thickness ratio and γ=3

depicted in Fig. 9. This figure shows that with increasing the amplitude of the external force the vibration amplitude increases uniformly for the $\Omega/\ \omega_{1,1}\leq 1$, while no bifurcation or jump is seen in the response path.In addition, with decreasing the external force from *f*=25 the response path is similar. However, at $\Omega/\ \omega_{1,1}$=1.02 and 1.03 the response paths have two bifurcation points. One jump occurs when the external force increases and the second one happens when the force amplitude decreases. Therefore, the response paths are different in these steps. This occurs because the nanosystem has nonlinear behavior. In addition, it can be seen that as the thickness ratio (*h/l*) decreases the

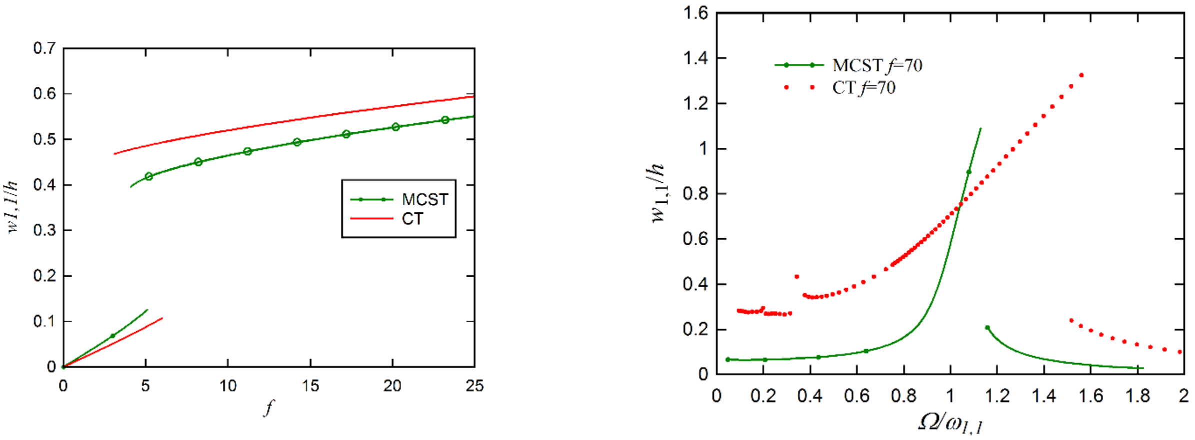

(a) (b)

Fig. 10 Force and frequency response predicted via the MCST and size-independent classical theory; γ=3, *h*/*l*=1

saddle-nodes bifurcations shift to higher forcing amplitudes.

The viscoelastic nanosystem force and frequency responses predicted via the classical continuum theory and the MCST are shown in Fig. 10 while the frequency ratio, $\Omega/\omega_{1,1}$, and forcing amplitude are 1.03 and 70. As the figure shows, the predicted responses of the two theories are very different. Particularly, for the MCST theory, the first saddle node bifurcation is at f=3.9 while for the classical theory, this occurs at f=3. Additionally, the MCST-based response amplitudes are much smaller than the values predicted by the CT at $f > 5$. In addition, it is seen that the classical theory predicts a stronger nonlinear hardening type behavior. Furthermore, there is a secondary resonance in the frequency response of the classical theory. However, there is no extra peak in the frequency response of the MCST. This figure highlights the importance of considering the small-scale effects proved by many experiments using the size-dependent theories such as the MCST instead of the size-independent continuum theory for prediction of the viscoelastic nanosystem resonance response with higher accuracy.

4. Conclusions

Current paper examined the time-dependent natural frequency and extra resonance in super-harmonic motions of a viscoelastic nano-resonator. The resonator was assumed as a nanoplate with simply supported boundary condition. Then, a new coupled size-dependent theory was developed for the nonlinear viscoelastic material with using the modified coupled stress theory. The viscoelastic material was considered to follow the Leaderman nonlinear integral. In order to predict the nanosystem oscillative behavior at relatively large deformations, the von-Karman nonlinearity was used. The virtual work was induced by the viscous forces obtained by applying the Leaderman integral. With incorporating the size-dependent potential energy, kinetic energy, and an external excitation force work based on the Hamilton's principle, the viscous work equation was balanced. The obtained coupled equations were a set of nonlinear second-order integro-differential partial equations. Theses equations were solved using the expansion theory, Galerkin method and the fourth-order Runge–Kutta technique. Then, the free vibration of the nanosystem was analyzed by performing the Hilbert–Huang Transform. Furthermore, the nonlinear forced vibration characteristics including the primary and secondary resonances due to the super-harmonic motions, of the nanosystem exposed to a distributed harmonic load were examined in the form of the frequency response, force response, Poincare map, phase portrait and fast Fourier transforms. Finally, the following results were obtained:

- Frequency analysis reveals that, (i) the natural frequency of the viscoelastic model unlike the elastic one decreased over the time. Therefore, this model predicts time-dependent natural frequencies unlike the elastic one. Moreover, the natural frequencies predicted by this model were smaller than those predicted by the elastic model; (ii) the fundamental natural frequencies predicted by the proposed model were larger than those predicted by the size-independent classical theory at each thickness ratio.
- The nonlinear frequency responses of the nanosystem revealed that: (i) the nanosystem dynamic behavior was a hardening type; (ii) stronger hardening behavior was predicted at bigger thickness ratios; (iii) super-harmonic frequencies existing in the response of the nanosystem cause to extra resonance specially at smaller frequency ratios;(iv) higher secondary resonances were seen at bigger forcing amplitudes; (v) with ignoring the small size-effects, the secondary resonance shifted significantly; (vi) the MCST predicted a minor hardening behavior and lower response amplitudes than the size-independent classical theory.
- The force-response analysis on the nanosystem showed that: (i) the nanosystem displayed continuous response path when the frequency ratios are smaller than one. However, there were jumps in the response path for the frequency ratios bigger than one; (ii) decreasing the thickness ratio (*h*/*l*) postponed the happening of saddle-nodes bifurcation; (iii). Taking into account the small-size effects causes shifting the saddle-node bifurcations to higher forcing amplitudes.

References

Aifantis, E.C. (1999), *Strain Gradient Interpretation of Size Effects*, Springer, Germany.

Ajri, M., Fakhrabadi, M.M.S. and A. Rastgoo (2018a), “Analytical solution for nonlinear dynamic behavior of viscoelastic nanoplates modeled by consistent couple stress theory”, *Latin American J. Solids Struct.*, **15**(9),1-23. http://doi.org/10.1590/1679-78254918.

Ajri, M., Fakhrabadi, M.M.S. and A. Rastgoo (2018b), “Primary and secondary resonance analyses of viscoelastic nanoplates based on strain gradient theory”, *J. Appl. Mech.*, **10**(10), 1850109.

Akbas, S.D. (2016), “Forced vibration analysis of viscoelastic nanobeams embedded in an elastic medium”, *Smart Struct. Syst.*, **18**(6), 1125-1143. http://doi.org/10.12989/sss.2016.18.6.1125.

Amabili, M. (2004), “Nonlinear vibrations of rectangular plates with different boundary conditions: theory and experiments”, *Comput. Struct.*, **82**(31-32), 2587-2605. https://doi.org/10.1016/j.compstruc.2004.03.077.

Asghari, M. (2012), “Geometrically nonlinear micro-plate formulation based on the modified couple stress theory”, *J. Eng. Sci.*, **51**, 292-309. https://doi.org/10.1016/j.ijengsci.2011.08.013.

Babaei, A., Noorani, M.R.S. and Ghanbari, A. (2017), “Temperature-dependent free vibration analysis of functionally graded micro-beams based on the modified couple stress theory”, *Microsyst. Technol.*, **23**(10), 4599-4610. https://doi.org/10.1007/s00542-017-3285-0.

Baghelani, M. (2016), “Design of a multi-frequency resonator for UHF multiband communication applications”, *Microsyst. Technol.*, **22**(10), 2543-2548. https://doi.org/10.1007/s00542-015-2639-8.

Braun, T., Barwich, V., Ghatkesar, M.K., Bredekamp, A.H., Gerber, C., Hegner, M. and Lang, H.P. (2005), “Micromechanical mass sensors for biomolecular detection in a physiological environment”, *Physical Review E*, **72**(3), 031907. https://doi.org/10.1103/PhysRevE.72.031907.

Budakian, R., Mamin, H. and Rugar, D. (2006), “Spin manipulation using fast cantilever phase reversals”, *Appl. Phys. Lett.*, **89**(11), 113113. https://doi.org/10.1063/1.2349311.

Christensen, R.M. and Freund, L. (1971), “Theory of viscoelasticity”, *J. Appl. Mech.*, **38**, 720.

Domaneschi, M., Limongelli, M.P. and Martinelli, L. (2013), “Vibration based damage localization using MEMS on a suspension bridge model”, *Smart Struct. Syst.*, **12**(6), 679-694. https://doi.org/10.12989/sss.2013.12.6.679.

Ehyaei, J. and Akbarizadeh, M.R. (2017), “Vibration analysis of micro composite thin beam based on modified couple stress”, *Struct. Eng. Mech.*, **64**(4), 403-411. https://doi.org/10.12989/sem.2017.64.4.403.

Ekinci, K., Huang, X. and Roukes, M. (2004), “Ultrasensitive nanoelectromechanical mass detection”, *Appl. Phys. Lett.*, **84**(22), 4469-4471. https://doi.org/10.1063/1.1755417.

Elwenspoek, M. and Jansen, H.V. (2004), *Silicon Micromachining*, Cambridge University Press, United Kingdom.

Fu, H. and Qian, Y. (2018), “Study on a Multi-Frequency Homotopy Analysis Method for Period-Doubling Solutions of Nonlinear Systems”, *J. Bifurcation Chaos*, **28**(04), 1850049. https://doi.org/10.1142/S0218127418500499.

Fu, Y. and Zhang, J. (2009), “Nonlinear static and dynamic responses of an electrically actuated viscoelastic microbeam”, *Acta Mechanica Sinica*, **25**(2), 211-218. https://doi.org/10.1007/s10409-008-0216-4.

Ghadiri, M., Mahinzare, M., Shafiei, N. and Ghorbani, K. (2017), “On size-dependent thermal buckling and free vibration of circular FG Microplates in thermal environments”, *Microsyst. Technol.*, **23**(10), 4989-5001. https://doi.org/10.1007/s00542-017-3308-x.

Ghayesh, M.H. and Amabili, M. (2012), “Nonlinear dynamics of axially moving viscoelastic beams over the buckled state”, *Comput. Struct.*, **112**, 406-421. https://doi.org/10.1016/j.compstruc.2012.09.005.

Ghayesh, M.H., Farokhi, H. and Amabili, M. (2013), “Nonlinear behaviour of electrically actuated MEMS resonators”, *J. Eng. Sci.*, **71**, 137-155. https://doi.org/10.1016/j.ijengsci.2013.05.006.

Ghayesh, M.H., Farokhi, H., Hussain, S., Gholipour, A. and Arjomandi, M. (2017), “A size-dependent nonlinear third-order shear-deformable dynamic model for a microplate on an elastic medium”, *Microsyst. Technol.*, **23**(8), 3281-3299. https://doi.org/10.1007/s00542-016-3096-8.

Gurtin, M.E. and Murdoch, A.I. (1975), “A continuum theory of elastic material surfaces”, *Arch Rat. Mech. Anal.*, **57**(4), 291-323. https://doi.org/10.1007/BF00261375.

Hashemi, S.H., Mehrabani, H. and Ahmadi-Savadkoohi, A. (2015), “Exact solution for free vibration of coupled double viscoelastic graphene sheets by viscoPasternak medium”, *Compos. Part B*, **78**, 377-383. https://doi.org/10.1016/j.compositesb.2015.04.008.

Huang, N.E., Shen, Z. and Long, S.R. (1999), “A new view of nonlinear water waves: the Hilbert spectrum”, *Annual Rev. Fluid Mech.*, **31**(1), 417-457.

Huang, N.E., Shen, Z., Long, S.R., Wu, M.C., Shih, H.H., Zheng, Q., Yen, N.C., Tung, C.C. and Liu, H.H. (1998). “The empirical mode decomposition and the Hilbert spectrum for nonlinear and non-stationary time series analysis”, *Proceedings of the Royal Society of London A: Mathematical, Physical and Engineering Sciences*. https://doi.org/10.1098/rspa.1998.0193.

Huang, X., Feng, X., Zorman, C., Mehregany, M. and Roukes, M. (2005), “VHF, UHF and microwave frequency nanomechanical resonators”, *New J. Phys.*, **7**(1), 247.

Huber, T.M., Abell, B.C., Mellema, D.C., Spletzer, M. and Raman, A. (2010), “Mode-selective noncontact excitation of microcantilevers and microcantilever arrays in air using the ultrasound radiation force”, *Appl. Phys. Lett.*, **97**(21), 214101. https://doi.org/10.1063/1.3521256.

Hwang, D.G., Chae, Y.M., Choi, N., Cho, I.J., Kang, J.Y. and Lee, S.H. (2017), “Label-free detection of prostate specific antigen (PSA) using a bridge-shaped PZT resonator”, *Microsyst. Technol.*, **23**(5), 1207-1214. https://doi.org/10.1007/s00542-015-2804-0.

Jamalpoor, A., Bahreman, M. and Hosseini, M. (2017), “Free transverse vibration analysis of orthotropic multi-viscoelastic microplate system embedded in visco-Pasternak medium via modified strain gradient theory”, *J. Sandwich Struct. Mater.*, https://doi.org/10.1177/1099636216689384.

JE., L. (1989), *Boundary Stabilization of Thin Plates*, SIAM, Philadelphia, USA.

Jiang, J.W., Wang, J.S. and Li, B. (2009), “Young’s modulus of graphene: a molecular dynamics study”, *Phys. Rev. B*, **80**(11), 113405. https://doi.org/10.1103/PhysRevB.80.113405.

Jomehzadeh, E., Noori, H. and Saidi, A. (2011), “The size-dependent vibration analysis of micro-plates based on a modified couple stress theory”, *Physica E: Low-dimensional Systems and Nanostructures*, **43**(4), 877-883. https://doi.org/10.1016/j.physe.2010.11.005.

Kalyanaraman, R., Rinaldi, G., Packirisamy, M. and Bhat, R. (2013), “Equivalent area nonlinear static and dynamic analysis of electrostatically actuated microstructures”, *Microsyst. Technol.*, **19**(1), 61-70. https://doi.org/10.1007/s00542-012-1621-y.

Karličić, D., Kozić, P. and Pavlović, R. (2014), “Free transverse vibration of nonlocal viscoelastic orthotropic multi-nanoplate system (MNPS) embedded in a viscoelastic medium", *Compos. Struct.*, **115**, 89-99. https://doi.org/10.1016/j.compstruct.2014.04.002.

Ke, L.-L., Wang, Y.-S., Yang, J. and Kitipornchai, S. (2012), "Free vibration of size-dependent Mindlin microplates based on the modified couple stress theory", *J. Sound Vib.*, **331**(1), 94-106. https://doi.org/10.1016/j.jsv.2011.08.020.

Khaniki, H.B. and Hosseini-Hashemi, S. (2017), "Dynamic response of biaxially loaded double-layer viscoelastic orthotropic nanoplate system under a moving nanoparticle", *J. Eng. Sci.*, **115**, 51-72. https://doi.org/10.1016/j.ijengsci.2017.02.005.

Lam, D.C., Yang, F., Chong, A., Wang, J. and Tong, P. (2003), "Experiments and theory in strain gradient elasticity", *J. Mech. Phys. Solids*, **51**(8), 1477-1508. https://doi.org/10.1016/S0022-5096(03)00053-X.

Leaderman, H. (1962), "Large longitudinal retarded elastic deformation of rubberlike network polymers", *Transac. Soc. Rheology*, **6**(1), 361-382. https://doi.org/10.1122/1.548932.

Lee, H.J., Zhang, P. and Bravman, J.C. (2005), "Stress relaxation in free-standing aluminum beams", *Thin Solid Films*, **476**(1), 118-124. https://doi.org/10.1016/j.tsf.2004.10.001.

Leng, H. and Lin, Y. (2011), "A MEMS/NEMS sensor for human skin temperature measurement", *Smart Struct. Syst.*, **8**(1), 53-67. https://doi.org/10.12989/sss.2011.8.1.053.

Li, M., Tang, H.X. and Roukes, M.L. (2007), "Ultra-sensitive NEMS-based cantilevers for sensing, scanned probe and very high-frequency applications", *Nature Nanotechnol.*, **2**(2), 114.

Liu, J., Zhang, Y. and Fan, L. (2017), "Nonlocal vibration and biaxial buckling of double-viscoelastic-FGM-nanoplate system with viscoelastic Pasternak medium in between", *Phys. Lett. A*, **381**(14), 1228-1235. https://doi.org/10.1016/j.physleta.2017.01.056.

López, G. (2013), "Diamond as a solid state quantum computer with a linear chain of nuclear spins system", *arXiv preprint arXiv:1310.0750*. https://doi.org/10.4236/jmp.2014.51009.

Lou, J. and He, L. (2015), "Closed-form solutions for nonlinear bending and free vibration of functionally graded microplates based on the modified couple stress theory", *Compos. Struct.*, **131**, 810-820. https://doi.org/10.1016/j.compstruct.2015.06.031.

Ma, H., Gao, X.L. and Reddy, J. (2011), "A non-classical Mindlin plate model based on a modified couple stress theory", *Acta Mechanica*, **220**(1-4), 217-235.

Mindlin, R. and Tiersten, H. (1962), "Effects of couple-stresses in linear elasticity", *Arch Rat. Mech. Anal.*, **11**(1), 415-448. https://doi.org/10.1007/BF00253946.

Mockensturm, E.M. and Guo, J. (2005), "Nonlinear vibration of parametrically excited, viscoelastic, axially moving strings", *J. Appl. Mech.*, **72**(3), 374-380.

Mohammadimehr, M., Navi, B.R. and Arani, A.G. (2015), "Free vibration of viscoelastic double-bonded polymeric nanocomposite plates reinforced by FG-SWCNTs using MSGT, sinusoidal shear deformation theory and meshless method", *Compos. Struct.*, **131**, 654-671. https://doi.org/10.1016/j.compstruct.2015.05.077.

Naik, A., Hanay, M., Hiebert, W., Feng, X. and Roukes, M. (2009), "Towards single-molecule nanomechanical mass spectrometry", *Nature Nanotechnol.*, **4**(7), 445.

Niyogi, A. (1973), "Nonlinear bending of rectangular orthotropic plates", *J. Solid. Struct.*, **9**(9), 1133-1139. https://doi.org/10.1016/0020-7683(73)90020-6.

Pan, Z. and Chen, J. (2017), "Measurements of pedestrian", *Struct. Eng. Mech.*, **63**(6).

Paolino, P. and Bellon, L. (2009), "Frequency dependence of viscous and viscoelastic dissipation in coated micro-cantilevers from noise measurement", *Nanotechnol.*, **20**(40), 405705.

Park, W.T., Han, S.C., Jung, W.Y. and Lee, W.H. (2016), "Dynamic instability analysis for S-FGM plates embedded in Pasternak elastic medium using the modified couple stress theory", *Steel Compos. Struct.*, **22**(6), 1239-1259. https://doi.org/10.12989/scs.2016.22.6.1239.

Qian, Y. and Fu, H. (2017), "Research for coupled van der Pol systems with parametric excitation and its application", *Zeitschrift für Naturforschung A*, **72**(11), 1009-1020. https://doi.org/10.1515/zna-2017-0249.

Qian, Y., Fu, H. and Guo, J. (2018), "Weakly resonant double Hopf bifurcation in coupled nonlinear systems with delayed freedback and application of homotopy analysis method", *J. Low Frequency Noise, Vib. Active Control*, ttps://doi.org/10.1177/1461348418765975.

Qian, Y. and Zhang, Y. (2017), "Optimal extended homotopy analysis method for Multi-Degree-of-Freedom nonlinear dynamical systems and its application", *Struct. Eng. Mech.,* **61**(1), 105-116. https://doi.org/10.12989/sem.2017.61.1.105.

Reddy, J. and Kim, J. (2012), "A nonlinear modified couple stress-based third-order theory of functionally graded plates", *Compos. Struct.*, **94**(3), 1128-1143. https://doi.org/10.1016/j.compstruct.2011.10.006.

Sato, M., Hubbard, B., Sievers, A., Ilic, B., Czaplewski, D. and Craighead, H. (2003), "Observation of locked intrinsic localized vibrational modes in a micromechanical oscillator array", *Physical Rev. Lett.*, **90**(4), https://doi.org/10.1103/PhysRevLett.90.044102.

Saulson, P.R. (1990), "Thermal noise in mechanical experiments", *Physical Review D*, **42**(8), 2437. https://doi.org/10.1103/PhysRevD.42.2437.

Setoodeh, A. and Rezaei, M. (2017), "Large amplitude free vibration analysis of functionally graded nano/micro beams on nonlinear elastic foundation", *Struct. Eng. Mech.*, **61**(2), 209-220. https://doi.org/10.12989/sem.2017.61.2.209.

Shim, S.-B., Imboden, M. and Mohanty, P. (2007), "Synchronized oscillation in coupled nanomechanical oscillators", *Science*, **316**(5821), 95-99. https://doi.org/10.1126/science.1137307.

Shinozuka, M., Chou, P.H., Kim, S., Kim, H., Karmakar, D. and Lu, F. (2010), "Non-invasive acceleration-based methodology for damage detection and assessment of water distribution system", *Smart Struct. Syst.*, **6**(6).

Smart, J. and Williams, J. (1972), "A comparison of single-integral non-linear viscoelasticity theories", *J. Mech. Phys. Solids*, **20**(5), 313-324. https://doi.org/10.1016/0022-5096(72)90027-0.

Su, Y., Wei, H., Gao, R., Yang, Z., Zhang, J., Zhong, Z. and Zhang, Y. (2012), "Exceptional negative thermal expansion and viscoelastic properties of graphene oxide paper", *Carbon*, **50**(8), 2804-2809. https://doi.org/10.1016/j.carbon.2012.02.045.

Tajaddodianfar, F., Yazdi, M.R.H. and Pishkenari, H.N. (2017), "Nonlinear dynamics of MEMS/NEMS resonators: analytical solution by the homotopy analysis method", *Microsyst. Technol.*, **23**(6), 1913-1926. https://doi.org/10.1007/s00542-016-2947-7.

Tang, Y.Q. and Chen, L.Q. (2012), "Parametric and internal resonances of in-plane accelerating viscoelastic plates", *Acta Mechanica*, **223**(2), 415-431. https://doi.org/10.1007/s00707-011-0567-y.

Teh, K.S. and Lin, L. (1999), "Time-dependent buckling phenomena of polysilicon micro beams", *Microelectronic. J.*, **30**(11), 1169-1172. https://doi.org/10.1016/S0026-2692(99)00081-6.

Toupin, R.A. (1962), "Elastic materials with couple-stresses", *Arch Rat. Mech. Anal.*, **11**(1), 385-414. https://doi.org/10.1007/BF00253945.

Tuck, K., Jungen, A., Geisberger, A., Ellis, M. and Skidmore, G. (2005), "A study of creep in polysilicon MEMS devices", *J. Eng. Mater. Technol.*, **127**(1), 90-96. https://doi.org/10.1016/j.physe.2014.11.007.

Wang, Y., Li, F.M. and Wang, Y.Z. (2015), "Nonlinear vibration of double layered viscoelastic nanoplates based on nonlocal theory", *Physica E: Low-dimensional Systems and Nanostructures*, **67**, 65-76. https://doi.org/10.1016/j.physe.2014.11.007.

Yan, X., Brown, W., Li, Y., Papapolymerou, J., Palego, C., Hwang, J. and Vinci, R. (2009), "Anelastic stress relaxation in gold films and its impact on restoring forces in MEMS devices", *J. Microelectromech. Syst.*, **18**(3), 570-576.

Yang, F., Chong, A., Lam, D.C.C. and Tong, P. (2002), "Couple stress based strain gradient theory for elasticity", *J. Solid. Struct.*, **39**(10), 2731-2743. https://doi.org/10.1016/S0020-7683(02)00152-X.

Yang, Y., Callegari, C., Feng, X., Ekinci, K. and Roukes, M. (2006), "Zeptogram-scale nanomechanical mass sensing", *Nano Lett.*, **6**(4), 583-586. https://doi.org/10.1021/nl052134m.

CC